Science and Technology Indonesia
e-ISSN:2580-4391 *p*-ISSN:2580-4405
Vol. 9, No. 2, April 2024

Research Paper

Improvement of Solubility Usnic Acid Loaded on Mesoporous Silica SBA-15 and Physicochemical Characterization

Lili Fitriani[1], Cindy Maynia Azzahra[1], Adhitya Jessica[1], Uswatul Hasanah[1], Erizal Zaini[1]*

[1]*Department of Pharmaceutics, Faculty of Pharmacy, Universitas Andalas, Kampus Limau Manis, Padang, 25175, Indonesia*
***Corresponding author**: erizal@phar.unand.ac.id*

Abstract
Usnic acid, a secondary metabolite of lichen *Usnea* sp., has several pharmacological activities, but it is poorly soluble in water. This study aimed to improve the solubility and dissolution rate of usnic acid loaded in mesoporous silica SBA-15 at a mass ratio of 1:1. and evaluate its physical stability. Physicochemical characterization was carried out via the nitrogen adsorption–desorption isotherm, differential scanning calorimetry (DSC), Fourier transform infrared (FTIR) spectroscopy, and powder X-ray diffraction (PXRD). Usnic acid-loaded SBA-15 was stored at 40 °C with various relative humidities (RH) and then analyzed by PXRD for the physical stability. Usnic acid adsorbed well in the pores of SBA-15, as shown by a decrease in the volume pore and surface area of SBA-15 according to the nitrogen adsorption. Moreover, usnic acid-SBA-15 showed a decrease in the degree of crystallinity according to PXRD analysis and no melting point based on DSC analysis. The FTIR spectrum of usnic acid–SBA-15 corresponds to the spectra of each raw material. The solubility of usnic acid increased 5.15 times after adsorbed on SBA-15. The dissolution rate also showed a significant increase ($p < 0.05$) from 19.51% to 84.27%. Usnic acid–SBA-15 was relatively stable at RH 75%. Thus, the adsorption of usnic acid on SBA-15 can increase its solubility, dissolution rate, and physical stability.

Keywords
Usnic Acid, SBA-15, Solubility, Dissolution Rate, Stability

Received: 5 November 2023, Accepted: 14 February 2024
https://doi.org/10.26554/sti.2024.9.2.251-259

1. INTRODUCTION

Lichen *Usnea* sp. has a secondary metabolite derived from dibenzofuran, which was isolated for the first time in 1844 and is known as usnic acid. Lichen, which contains a considerable amount of usnic acid, has been extensively studied by scientists and is widely available commercially (Fitriani et al., 2018a). In the health sector, usnic acid has been used in medicines, owing to its many pharmacological activities, such as antiviral (Sokolov et al., 2012), anticancer (Mayer et al., 2005), antiproliferative (Campanella et al., 2002), antipyretic, analgesic (Okuyama et al., 1995), antioxidant (Behera et al. (2005)), and anti-inflammatory (Vijayakumar et al., 2000) activities. However, usnic acid has a solubility of less than 0.01 g in 100 mL of water at 25 °C, which is practically insoluble in water (Fitriani et al., 2018a). Based on the Biopharmaceutical Classification System (BCS), usnic acid is included as a BCS class II, due to low solubility but high permeability. This has an impact on the low absorption of usnic acid in the gastrointestinal tract, thus limiting its bioavailability (Brugnoli et al., 2024). Therefore, higher doses are needed to achieve its therapeutic effect (Holford and Sheiner, 1981). Meanwhile, in vitro, the low solubility of a substance in water will affect several stages of product development, including dissolution, may change the drug activity, and may even lead to toxicity (Maleki et al., 2017).

The limitations of the physicochemical properties of usnic acid, particularly its solubility, have an impact on its limited pharmacological effects, thus promoting investigations to increase its solubility (Brugnoli et al., 2024). Many methods have been confirmed to increase the solubility and dissolution rate of usnic acid, such as solid dispersion with Poloxamer 188 (Brugnoli et al., 2024), PVP K-30 and PEG 6000 (Chairunisa et al., 2022), and HPMC 2910 (Fitriani et al., 2018a). In addition, inclusion complex methods with β-cyclodextrin (Lira et al., 2009), multi component crystals (Douglas A. Araújo et al., 2019), and particle size reduction (milling) (Zaini et al., 2016) have been reported. However, these methods have limitations. Solid dispersions are difficult to produce on a large scale, and the products have low physical and chemical stability. Agglomeration occurs during post-grinding storage, and the resulting particle size is unstable, resulting in varying dissolution rates for the particle size reduction method (Shen et al., 2010). Meanwhile, the inclusion complex with β-cyclodextrin has

limitations in terms of size and requires greater costs (Maleki et al., 2017).

Alternatively, one of the methods effective at increasing the solubility of active drug substances and guaranteed stability is adsorption, in which this method has attracted great interest due to its benefit such as simple for application in many fields including pharmaceutical preparation or medicines (Palapa et al., 2023). The active compound can be adsorbed in the surface of mesoporous including silica which have been approved generally recognized as safe materials (GRAS) by food and drug administration (FDA) (Tng and Low, 2023). The pore size distribution of mesoporous silica can be varied and adjusted between 2 and 50 nm. In addition, silica-based mesopores have a high specific surface area, resulting in a higher adsorption potential, large pore volume, and surface-containing silanol groups with the function of modifying drug release (Shen et al., 2010). The most frequently used types of mesoporous silica are Mobile Composition of Matter-41 (MCM-41) and Santa Barbara Amorphous-15 (SBA-15), with a hexagonal two-dimensional arrangement. The other type is the Mobile Composition of Matter-48 (MCM-48), which has a cubic three-dimensional arrangement (Maleki et al., 2017). Mesoporous SBA-15 silica with a pore wall thickness of 4 nm and a pore diameter of 10 nm is more stable than mesoporous MCM-41 silica with only a 1-nm pore wall thickness and 4-nm pore diameter (Galarneau et al., 2007). Mesoporous SBA-15 uses an amphiphilic triblock copolymer from poly(ethylene oxide)-poly(propylene oxide), such as Pluronic P123, as a structure-directing reagent in highly acidic media (Vinu et al., 2006).

In this study, usnic acid was adsorbed on SBA-15, and solubility and dissolution rate tests were conducted. In addition, physical stability tests were carried out to ensure that adsorbed usnic acid is physically stable. The SBA-15 mesopores and usnic acid – loaded SBA 15 that were prepared then characterized by nitrogen adsorption–desorption isotherm, powder X-ray diffraction (PXRD), Fourier transform infrared (FTIR) spectroscopy, differential scanning calorimetry (DSC), and scanning electron microscopy (SEM)

2. EXPERIMENTAL SECTION

2.1 Materials

Usnic acid and tetraethyl orthosilicate (TEOS) were purchased from the Tokyo Chemical Industry (TCI) (Japan). Pluronic P123 and sodium chloride were provided by Sigma Aldrich (USA). Sodium lauryl sulfate (SLS), chloroform pro analysis (p.a) and hydrochloric acid were purchased from Merck (Germany). All materials were used without further purification.

2.2 Preparation of Mesoporous Silica SBA-15

The synthesis of SBA-15 was carried out by preparing TEOS : NaCl : HCl : H_2O : Pluronic P123 in a molar ratio of 1 : 6 : 6 : 166 : 0.02, respectively. Pluronic P123 and NaCl were mixed, and H_2O and 2 M HCl were added. The mixture was stirred using a magnetic stirrer at 300 rpm for 24 h at room temperature. Then, TEOS was added, and the stirring speed was increased up to 700 rpm for 3 h. The mixture then was heated in the oven at 80 °C for 24 h, which is a hydrothermal process. The precipitate that formed was filtered using filter paper, rinsed using distilled water, and then dried at 50 °C for approximately 14 h. The last step was to remove the surfactant via a calcination process at 550 °C for 4 h; then, SBA-15 mesoporous powder was obtained (Yu et al., 2001; Liu et al., 2023)

2.3 Adsorption of Usnic Acid in Mesoporous Silica SBA-15

The adsorption of usnic acid in mesoporous SBA-15 was carried out at a ratio of 1:1 (w/w). 200 mg of usnic acid was dissolved in 10 ml chloroform p.a. Then, SBA-15 powder was added to the usnic acid solution. The mixture was stirred with a magnetic stirrer at a temperature of 80 °C and a speed of 300 rpm. Stirring was continued until the solvent evaporated, and SBA-15 usnic acid powder was obtained. The dried usnic acid loaded in SBA-15 was then kept in a desiccator.

2.4 Nitrogen Adsorption–desorption Isotherm

SBA-15 and usnic acid – loaded SBA-15 samples were tested using an adsorption–desorption isotherm with nitrogen gas using the BET surface area and a pore-size analyzer (Quantachrome Novatouch LX-4, USA). The experiment was carried out at a degassing temperature of 150 °C. The results obtained included the P/Po value and the BET transformation value [1/W(P/Po)] for calculating the area.

2.5 DSC analysis

The thermodynamic properties of usnic acid, SBA-15, and usnic acid-loaded SBA-15 were analyzed by thermal analysis via DSC on a Shimadzu DSC-60 Plus (Japan) which set in the temperature range of 25–250 °C with a heating speed of 10 °C/min.

2.6 PXRD analysis

PXRD analysis was performed for usnic acid, SBA-15, and usnic acid-loaded SBA-15 using a diffractometer (PAN analytical MPD PW3040/60 type X'Pert Pro, The Netherlands). The measurement conditions included a Cu metal target and Kα filter. In the testing process, a generator setting was used with a voltage of 40 kV, a current of 30 mA, and in the 2θ range of 5–50°.

2.7 FTIR Spectroscopy

Samples of usnic acid, SBA-15, and usnic acid-loaded SBA-15 were analyzed to identify the functional groups in each sample using an FTIR spectrophotometer (Shimadzu IR-Tracer-100-AH, Japan) by dispersing the sample on a KBr plate that was compressed under high pressure. The absorption spectrum was recorded at 4000–500 cm^{-1}.

2.8 SEM Analysis

SEM analysis was performed for samples of usnic acid, SBA-15, and usnic acid-loaded SBA-15 (Hitachi Flexsem 100, Japan). Samples in powder form were placed in an aluminum sample

holder and coated with gold with a thickness of 10 nm. The SEM was programmed at 5 kV, and the samples were observed at various magnifications.

2.9 Entrapment Efficiency

Entrapment efficiency was performed for usnic acid-loaded SBA-15 in a ratio of 1 : 1 (w/w), by weighing a sample equivalent to 10 mg of usnic acid. Then, the sample was dissolved in chloroform for analysis. The amount of usnic acid absorbed in SBA-15 was determined using a UV–Vis spectrophotometer (Shimadzu UV-1700, Japan) at the maximum wavelength (283.6 nm). Entrapment efficiency (EE) can be calculated with the following equation:

$$\%EE = \frac{Usnic\ Acid\ Mass\ Adsorbed}{Usnic\ Acid\ Mass\ Used} \times 100\%$$

2.10 Solubility Test

Solubility tests were carried out on intact usnic acid and usnic acid-loaded SBA-15 samples. The excess amount of sample was dissolved in 100 mL of CO_2-free distilled water. The test was conducted for 24 h using an orbital shaker at room temperature. Then, the sample was filtered through a 0.45-µm membrane filter, and the absorption of the filtrate was measured using a UV–Vis (Shimadzu UV-1700, Japan) spectrophotometer at 289.6 nm. The test was carried out in triplicate.

2.11 Dissolution Test

The dissolution rate profile was carried out on intact usnic acid and usnic acid-loaded SBA-15 samples using a type II dissolution apparatus (paddle type) (Hanson SR8-Plus, USA). The dissolution flask was filled with 900 mL of CO_2-free distilled water medium and 0.1% w/v SLS. The dissolution apparatus was set at 37 ± 0.5 °C with a speed of 50 rpm. The sample was weighed equivalent to 10 mg of usnic acid. Samples were pipetted (5 mL) at intervals of 5, 10, 15, 30, 45, and 60 min. The sample that was pipette was replaced using a fresh dissolution medium using the same conditions (volume and temperature). Each sample was placed into a vial and analyzed via UV–Vis spectrophotometry (Shimadzu UV-1700, Japan) at 289.4 nm.

2.12 Physical Stability Test

A physical stability test was carried out for usnic acid–SBA-15. The samples were stored in a climatic chamber (Memmert HPPeco, Germany), and the relative humidity (RH) was set at 75%, 85%, and 90% at 40 °C for 2 weeks (Zaini et al., 2016). Then, the physical stability of the usnic acid was investigated via PXRD analysis.

2.13 Data Analysis

The solubility and dissolution rate results were analyzed statistically with one-way ANOVA using SPSS 26 (IBM, USA).

3. RESULTS AND DISCUSSION

A nitrogen adsorption–desorption isotherm was used to determine the synthesized SBA-15 pores. At low relative pressure (approximately zero), the adsorption volume of nitrogen increases as the pressure increases. This indicated that the mesopores are filled with nitrogen and the surface will be covered, thus forming a monolayer, and at the end of the curve, a slope will form, indicating that the first multilayer has formed as illustrated in Figure 1.

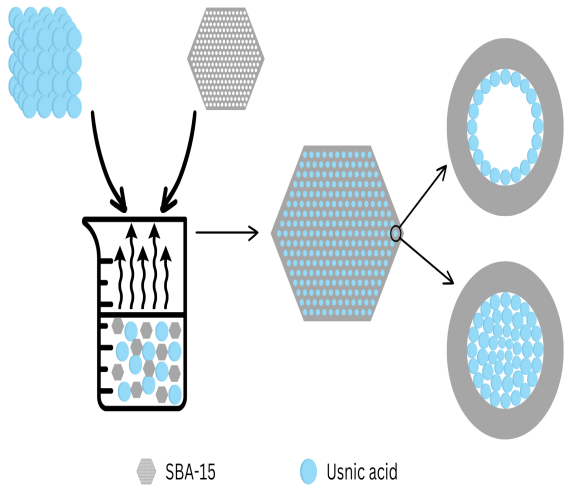

Figure 1. Schematic of Usnic Acid Loaded on Mesoporous SBA-15

The results of the nitrogen adsorption–desorption isotherm analysis revealed that the pore size of SBA-15 matched the mesoporous range of 2–50 nm. This can be confirmed by the formation of a type IV isotherm curve, with the presence of a hysteresis loop at a relative pressure of 0.4–0.8, as shown in the Figure 2 (Maleki and Hamidi, 2015). This characterization must be maintained when adsorption is complete, indicating that the mesoporous material is still present and not damaged after adsorption (Ahern et al., 2013). The hysteresis loop is formed because the number of nitrogen molecules that are desorbed is less than the number of nitrogen molecules that are adsorbed, even though the relative pressure P/Po is the same (Fitriani et al., 2022).

Table 1. The Result of Pore Characterization of SBA-15 and Usnic Acid – Loaded SBA15

	SBA-15	Usnic acid-loaded SBA 15
Surface Area (m^2/g)	650.44	177.30
Pore Volume ($\times 10^{-1}$ cm^3/g)	8.931	2.262
Pore Size (nm)	R = 2.74 or D = 5.49	R= 2.95 or D = 5.91

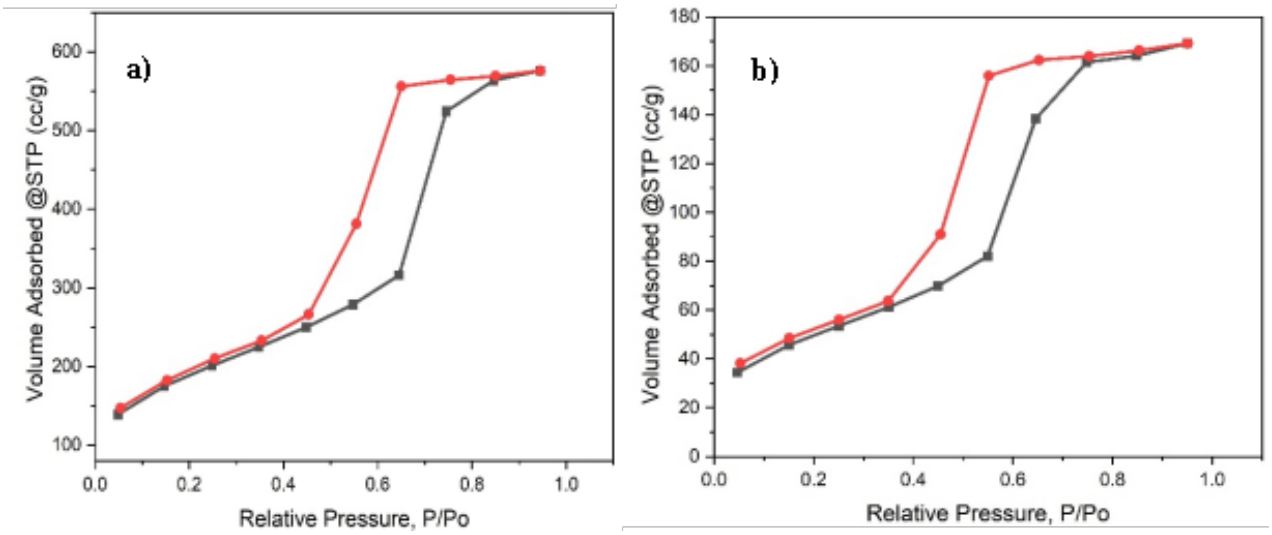

Figure 2. Isothermic Curves of a) SBA-15 and b) Usnic Acid-SBA-15

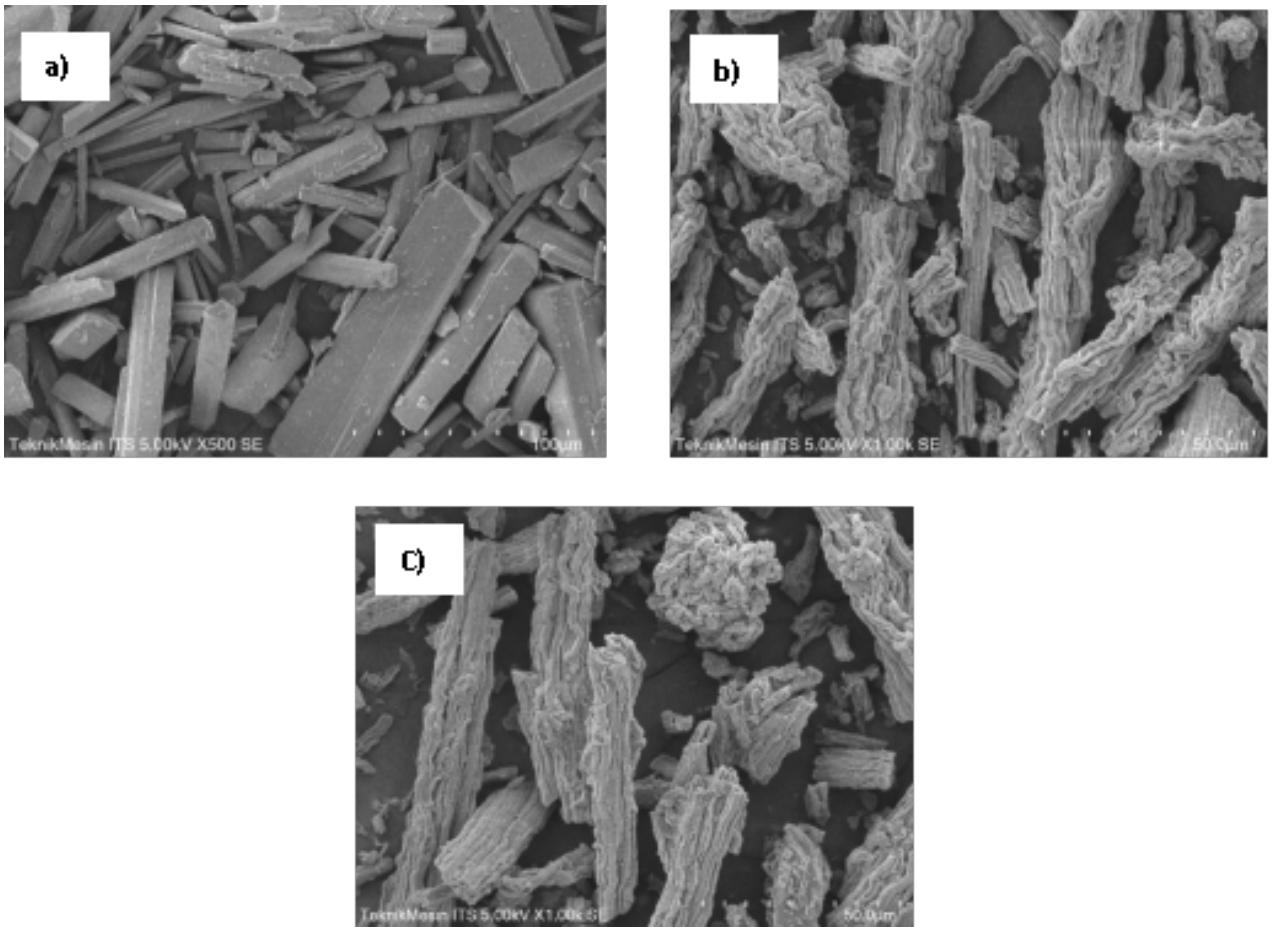

Figure 3. Morphology of a) Usnic Acid, b) SBA-15, and c) Usnic Acid-SBA-15

Based on the surface area and pore volume analysis shown in Table 1, the pores of SBA-15 were well filled with usnic acid after adsorption. This result shows the smaller surface area and pore volume of SBA-15 after adsorption. The surface area decreased from 650.443 m^2/g to 177.303 m^2/g, and the pore volume decreased from 8.93193×10^{-1} cm^3/g to 2.262255

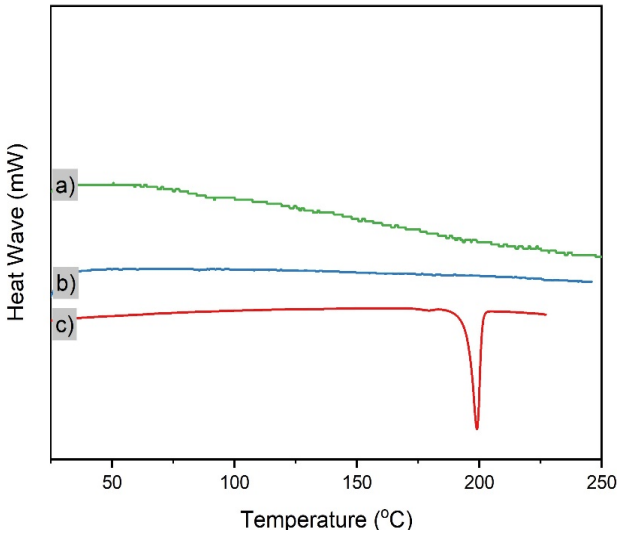

Figure 4. Thermogram of a) Usnic Acid-SBA-15, b) SBA-15, and c) Usnic Acid

$\times 10^{-1}$ cm^3/g. However, the pore size of SBA-15 increased slightly after adsorption owing to the complete filling of the small mesopores. The pore diameters of SBA-15 increased after it was adsorbed with a high concentration of active substance because the substance filled the smaller pores, while there was still free space left in the larger pores (Heikkilä et al., 2007). However, the increase in pore diameter was not significant, indicating that the pore shape before and after adsorption did not change, which was also observed in the SEM analysis. SEM shows the morphology of a solid material. The SEM images (Fig. 3) showed that usnic acid has a needle-shaped crystal morphology (Figure 3a). Meanwhile, SBA-15 (Figure 3b) has an aggregated rod-shaped morphology with uniform lengths (Adrover et al., 2020). The morphology of usnic acid –loaded SBA 15 (Figure 3c) was similar to that of SBA-15, which indicates that usnic acid can be adsorbed properly and there is no visible usnic acid blocking the pores or outside the SBA-15 pores. Therefore, only SBA-15 could be observed because the usnic acid was adsorbed into the pores of SBA-15. The morphology results were confirmed by the thermal characterization via DSC, which showed that there were no sharp endothermic peaks of usnic acid in the thermogram. This indicated that usnic acid was well adsorbed in the mesoporous material in an amorphous state and that usnic acid that was still outside the pores was almost invisible. However, some were not adsorbed in the pores, as shown in the PXRD (Shen et al., 2010). As shown in Figure 4, usnic acid showed an endothermic peak at 203.12 °C, which is the melting point of usnic acid. There was no endothermic peak in the SBA-15 thermogram, which indicated that SBA-15 was an amorphous solid material. This is similar to the thermogram of the usnic acid – loaded SBA 15, which also did not show an endothermic peak. In usnic acid adsorbed on SBA-15, there was a "suppression of crystallization" or obstruction of the crystallization process of the active substance adsorbed on SBA-15. Thus, usnic acid was transformed to a non-crystalline form and could return to the crystalline state (amorphization process). The active substance adsorbed in mesoporous silica will experience a change in thermodynamic properties compared to the intact one. If a substance is adsorbed into a porous material with a limited pore size, it will be prevented from forming a crystal lattice (Van Speybroeck et al., 2009). In this case, the pore diameter of SBA-15 is only 5.49 nm; thus, the crystallization process of usnic acid trapped in it will be hindered.

Functional group analysis via FTIR was performed for usnic acid, SBA-15, and the usnic acid-loaded SBA-15 sample (Figure 5). Usnic acid shows a C=O bond at 1687.71 cm^{-1}, a C–H bond at 1442.75 cm^{-1}, a C=C bond at 1616.35 cm^{-1}, and an O–H bond at 3091.89 cm^{-1}. The results were similar to those in previous studies, which showed C=O and C=C bonds at 1691.60 cm^{-1} and 1610.36 cm^{-1} (Fitriani et al., 2018b). In the SBA-15 spectrum, at 3523.95 cm^{-1}, the peak indicated the presence of O–H groups. At 422.41 cm^{-1}, we observed the presence of Si−O−Si bonds. In addition, the peak at 1045.42 cm^{-1} showed asymmetric Si–O–Si bending, and that at 804.32 cm^{-1} showed symmetric Si–O–Si stretching. Asymmetric Si–O–Si stretching occurs at 1090–1103 cm^{-1}; however, symmetric Si–O–Si stretching is shown at 801 cm^{-1} (Thahir et al., 2019). After the adsorption of usnic acid on SBA-15, the FTIR spectrum of usnic acid–SBA-15 showed a superimposition of the characteristic spectrum of intact usnic acid with that of SBA-15. This confirmed that usnic acid adsorbed well on SBA-15, although there was a slight shift in the peak. C=O, C=C, C–H, Si–O–Si bending, Si–O–Si asymmetric bending, Si–O–Si symmetric stretching, and O–H bonding are represented by 1691.57 cm^{-1}; 1631.78 cm^{-1}; 1456.26 cm^{-1}; 439.77 cm^{-1}; 1037.70 cm^{-1}; 800.46 cm^{-1} and 3714.90 cm^{-1}, respectively. This change is related to the hydrogen bonding between Si–OH and the usnic acid functional group (Maleki and Hamidi, 2015). Therefore, based on functional group analysis with FTIR, the structures of usnic acid and SBA-15 did not change after the adsorption process occurred.

PXRD is typically used to identify and characterize crystalline materials. Each crystalline material has a unique diffraction pattern due to the arrangement of its atoms in the lattice (Zaini et al., 2016). The diffractogram for usnic acid shows a sharp and distinctive peak, which means that usnic acid is a crystalline solid in nature. The specific diffraction crystal peak of usnic acid is shown at 2θ positions of 10.35, 12.77, 14.67, 18.58, 19.90, 25.01, 26.30, 29.49, and 44.21. However, SBA-15 demonstrated a diffuse diffractogram pattern, which indicated that SBA-15 is an amorphous solid. After usnic is adsorbed on mesoporous SBA-15, the peaks of usnic acid crystals are still detected in the diffractogram of usnic acid – loaded SBA-15, although the intensity is lower than the intact crystal, as shown in Figure 6. This phenomenon occurs because most of the usnic acid is already in an amorphous state, but the rest of it has not been adsorbed into SBA-15 and is still in the

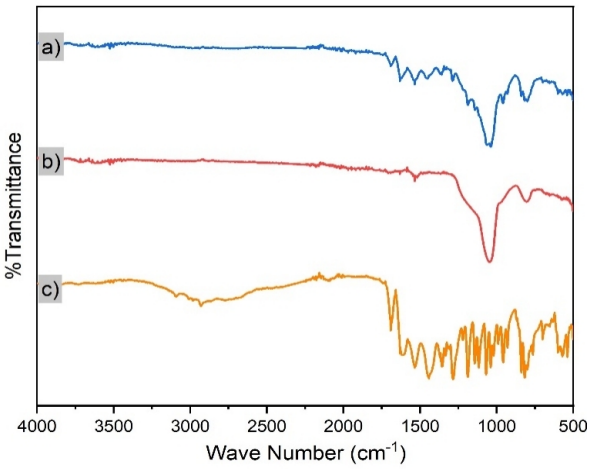

Figure 5. Diffractogram of a) Usnic Acid – Loaded SBA-15, b) SBA-15, and c) Usnic Acid

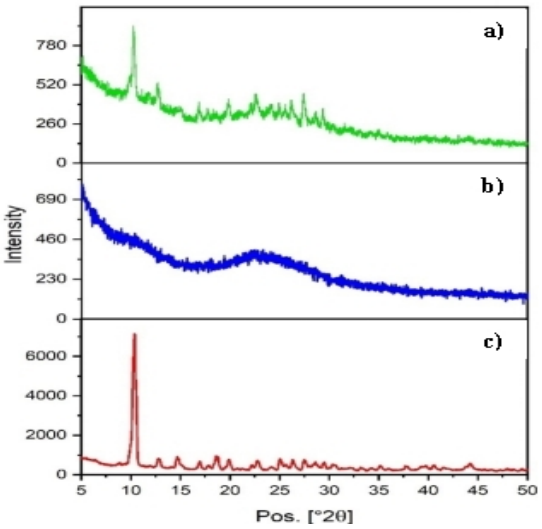

Figure 6. Diffractogram of a) Usnic Acid – Loaded SBA-15, b) SBA-15, and c) Usnic Acid

crystalline state. Consequently, usnic acid crystals that were still outside the pores were detected by PXRD. The results were similar to those in a carbamazepine study. Carbamazepine crystal peaks were still detectable when carbamazepine was adsorbed at 30% onto SBA-15. However, when carbamazepine was only 10% and 20% adsorbed, the crystal peaks disappeared (Wang et al., 2012). In another study, ibuprofen was adsorbed onto SBA-15 at a mass ratio of 1:1, and the diffraction peak of ibuprofen crystals on the diffractogram still appeared even though adsorption occurred according to the PXRD analysis. The phenomenon, which is similar to this study, showed that ibuprofen still had peak intensity likely owing to the formation of ibuprofen crystals on the pore surface during solvent removal by the evaporation process (Shen et al., 2010).

The entrapment efficiency of usnic acid in mesoporous

Table 2. Solubility Data of Usnic Acid and Usnic Acid-SBA-15

Sample	Solubility ± SD (mg/100 mL)	Solubility Enhancement
Intact Usnic Acid	0.60 ± 0.03	-
Usnic Acid -SBA-15	3.10 ± 0.14	5.15 times

SBA-15 is 88.58% ± 1.31. Effective adsorption of a drug molecule will occur if the entrapment efficiency is close to 100%. However, the proportion of entrapment efficiency is categorized as good if the value is greater than 60% (Supraba et al., 2021). The loss of usnic acid by as much as 11.41% in the adsorption process was likely due to some processes before the measurements. Adsorption of usnic acid in SBA-15, which was at 88.58%, could increase the solubility and dissolution rate of usnic acid in CO_2-free distilled water, as shown in Table 2. Previous research showed that albendazole, which is only adsorbed at approximately 30.3% in SBA-15, can increase the solubility and dissolution rate of albendazole – loaded SBA 15 (Adrover et al., 2020). In this study, the solubility of usnic acid increased 5.153 times when it was adsorbed on mesoporous silica SBA-15. The increase in solubility was likely due to the inhibition of the recrystallization process of the adsorbed usnic acid. The formation of hydrogen bonds through surface silanol groups and the limited space in the mesoporous SBA-15 channel is because of the thick and rigid SBA-15 framework (Letchmanan et al., 2017). Therefore, usnic acid that has been adsorbed on mesopores has a higher solubility compared to its crystalline form.

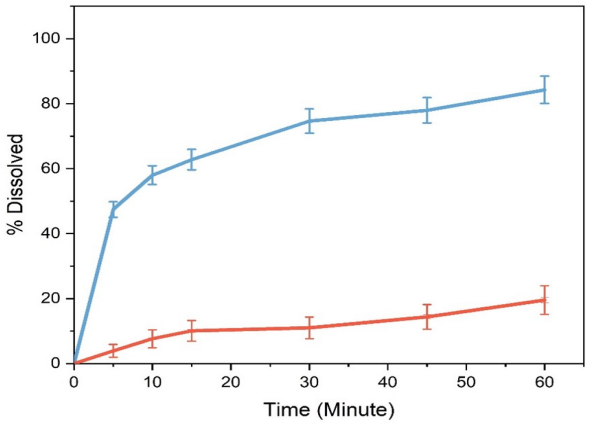

Figure 7. Dissolution Rates Profile of (a) Usnic Acid and (b) Usnic Acid – Loaded SBA 15

The percentage of dissolved usnic acid in CO_2-free distilled water with an additional 0.1% w/v SLS is shown in Figure 7. The amount of usnic acid dissolved in SBA-15 was greater than in the intact usnic acid. The dissolutions of intact usnic acid and usnic acid-loaded SBA-15 after 5 min were 3.90 ± 0.434 and 47.40 ± 2.62, respectively. Dissolution of both samples

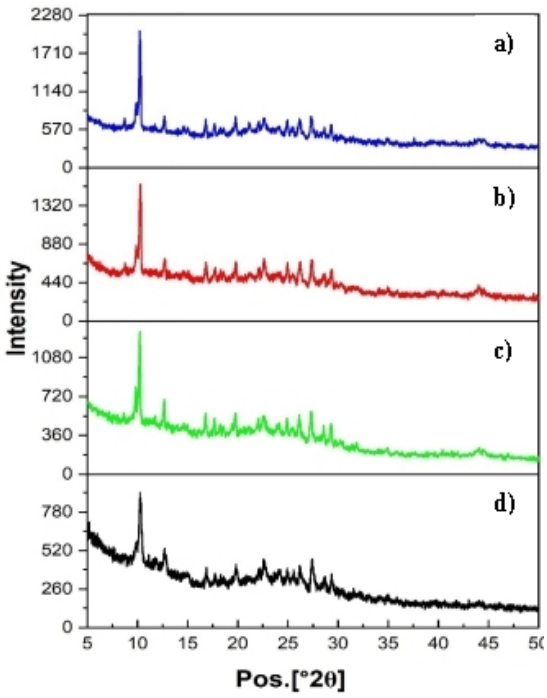

Figure 8. Diffractogram of Usnic Acid – Loaded SBA15 at a) RH 90% , b) RH 85%, c) RH 75%, and d) Usnic Acid – Loaded SBA15

continued to increase over time until 60 min, reaching 19.51 ± 1.56 and 84.26 ± 1.84 for usnic acid and usnic acid loaded SBA-15, respectively. According to the Noyes–Whitney equation, the dissolution rate depends on several factors, such as the solubility and surface area of the active substance (Gao et al., 2021). Usnic acid adsorbed on SBA-15 has a solubility 5.15 times higher than pure usnic acid. In addition, the small particle size makes better contact between the active substance and the dissolution medium. Its large specific surface area can also increase the wettability of hydrophobic drugs (Wang et al., 2012). The pore structure of the SBA-15 mesopores exerts a restrictive effect that does not allow crystals to form. Crystals that have high lattice energy limit the solubility process. The formation of the amorphous phase of usnic–SBA-15 acid, resulting in a reduction in lattice energy from usnic acid solids, is also the cause of increased dissolution of usnic acid when it is adsorbed on SBA-15 (Dadej et al., 2021). In another study, the active substance dispersed in an amorphous state in the SBA-15 pores, which interacted with the silanol group on the mesoporous surface, consequently increasing the dissolution rate of the active substance. Increased dissolution of the active substance due to adsorption on SBA-15 can increase the absorption and bioavailability of the insoluble drug in the body (Wang et al., 2012). Physical stability tests on usnic acid-loaded SBA 15 were conducted in a climatic chamber at RH values of 75%, 85%, and 90%, respectively, at 40 °C for 2 weeks. PXRD analysis was used to evaluate the solid-state properties of usnic acid-loaded SBA-15. Figure 8d shows the PXRD pattern of usnic acid-loaded SBA-15 before storage and after storage at different RH values (Figure 8 a-c). The diffractogram of usnic acid did not considerably change. This indicated that the transformation of crystalline usnic acid to another form was ruled out at high RH. In general, usnic acid – loaded SBA-15 was physically stable upon storage at high RH.

4. CONCLUSIONS

Usnic acid can be adsorbed in SBA-15 silica mesopores according to nitrogen adsorption–desorption isotherm analysis, SEM, DSC, PXRD, and DSC. The adsorption of usnic acid on SBA-15 can increase the solubility of usnic acid by 5.15 times and increase the dissolution rate of usnic acid from 19.51% to 84.26% within 60 min. Usnic acid–SBA-15 is also relatively stable if stored at high RH.

5. ACKNOWLEDGMENT

The authors would like to thank Faculty of Pharmacy Universitas Andalas for granting this research under Riset Dasar (No. 04/UN.16.10/D/PJ.01/2023).

REFERENCES

Adrover, M. E., M. Pedernera, M. Bonne, B. Lebeau, V. Bucalá, and L. Gallo (2020). Synthesis and Characterization of Mesoporous SBA-15 and SBA-16 As Carriers to Improve Albendazole Dissolution Rate. *Saudi Pharmaceutical Journal*, **28**(1); 15–24

Ahern, R. J., J. P. Hanrahan, J. M. Tobin, K. B. Ryan, and A. M. Crean (2013). Comparison of Fenofibrate-Mesoporous Silica Drug-Loading Processes for Enhanced Drug Delivery. *European Journal of Pharmaceutical Sciences*, **50**(3-4); 400–409

Behera, B., N. Verma, A. Sonone, and U. Makhija (2005). Antioxidant and Antibacterial Activities of Lichen Usnea Ghattensis in Vitro. *Biotechnology letters*, **27**; 991–995

Brugnoli, B., G. Perna, S. Alfano, A. Piozzi, L. Galantini, E. Axioti, V. Taresco, A. Mariano, A. Scotto d'Abusco, and S. Vecchio Ciprioti (2024). Nanostructured Poly-l-lactide and Polyglycerol Adipate Carriers for the Encapsulation of Usnic Acid: A Promising Approach for Hepatoprotection. *Polymers*, **16**(3); 427

Campanella, L., M. Delfini, P. Ercole, A. Iacoangeli, and G. Risuleo (2002). Molecular Characterization and Action of Usnic Acid: A Drug That Inhibits Proliferation of Mouse Polyomavirus in Vitro and Whose Main Target Is RNA Transcription. *Biochimie*, **84**(4); 329–334

Chairunisa, U., D. K. Haryati, R. Wahyuni, I. Makmur, S. Effendy, R. D. Yetti, A. Eriadi, H. S. K. Uyun, D. D. A. Bakhtra, A. Halim, and M. Fadhilah (2022). Increasing the Dissolution Rate of USNAC PVP K-30 and PEG6000 Solid Dissolution Using Solution Method. *International Journal of Research Publication and Reviews*, **3**(8); 458–463

Dadej, A., A. Woźniak Braszak, P. Bilski, H. Piotrowska Kempisty, M. Józkowiak, M. Geszke Moritz, M. Moritz, D. Dadej,

and A. Jelińska (2021). Modification of the Release of Poorly Soluble Sulindac with the APTES-Modified SBA-15 Mesoporous Silica. *Pharmaceutics*, **13**(10); 1693

Douglas A. Araújo, H., J. G. Silva Júnior, J. R. Saturnino Oliveira, M. Helena ML Ribeiro, M. C. Barroso Martins, M. A. Cavalcanti Bezerra, A. Lima Aires, M. CP Azevedo Albuquerque, M. R. Melo-Júnior, and N. T. Pontes Filho (2019). Usnic Acid Potassium Salt: Evaluation of the Acute Toxicity and Antinociceptive Effect in Murine Model. *Molecules*, **24**(11); 2042

Fitriani, L., I. Afriyanti, F. Ismed, and E. Zaini (2018a). Solid Dispersion of Usnic acid-HPMC 2910 Prepared by Spray drying and Freeze drying Techniques. *Oriental Journal of Chemistry*, **34**(4)

Fitriani, L., H. Azizah, U. Hasanah, and E. Zaini (2022). Enhancement of Curcumin Solubility and Dissolution by Adsorption in Mesoporous SBA-15. In *International Conference on Contemporary Science and Clinical Pharmacy*. page 61

Fitriani, L., E. Rismawati, S. Umar, and E. Zaini (2018b). Solid Dispersion of Usnic Acid-PVP K30 and Evaluation of Antioxidant Activity. *Rasayan Journal of Chemistry*, **11**; 1643–1648

Galarneau, A., M. Nader, F. Guenneau, F. Di Renzo, and A. Gedeon (2007). Understanding the Stability in Water of Mesoporous SBA-15 and MCM-41. *The Journal of Physical Chemistry C*, **111**(23); 8268–8277

Gao, Y., B. Glennon, Y. He, and P. Donnellan (2021). Dissolution Kinetics of a BCS Class II Active Pharmaceutical Ingredient: Diffusion-Based Model Validation and Prediction. *ACS Omega*, **6**(12); 8056–8067

Heikkilä, T., J. Salonen, J. Tuura, N. Kumar, T. Salmi, D. Y. Murzin, M. Hamdy, G. Mul, L. Laitinen, and A. M. Kaukonen (2007). Evaluation of Mesoporous TCPSi, MCM-41, SBA-15, and TUD-1 Materials as API Carriers for Oral Drug Delivery. *Drug Delivery*, **14**(6); 337–347

Holford, N. H. and L. B. Sheiner (1981). Understanding the Dose-Effect Relationship: Clinical Application of Pharmacokinetic-Pharmacodynamic Models. *Clinical Pharmacokinetics*, **6**(6); 429–453

Letchmanan, K., S.-C. Shen, W. K. Ng, and R. B. Tan (2017). Dissolution and Physicochemical Stability Enhancement of Artemisinin and Mefloquine Co-Formulation Via Nano-Confinement with Mesoporous SBA-15. *Colloids and Surfaces B: Biointerfaces*, **155**; 560–568

Lira, M. C., M. S. Ferraz, D. G. da Silva, M. E. Cortes, K. I. Teixeira, N. P. Caetano, R. D. Sinisterra, G. Ponchel, and N. S. Santos-Magalhaes (2009). Inclusion Complex of Usnic Acid with β-Cyclodextrin: Characterization and Nanoencapsulation into Liposomes. *Journal of Inclusion Phenomena and Macrocyclic Chemistry*, **64**; 215–224

Liu, X., N. Liu, X. Li, X. Li, B. Hu, and S. He (2023). Surface Properties and Microstructures of Al-SBA-15 under Different Temperature Calcinations in Relation to Adsorption Performance. *The Journal of Physical Chemistry C*, **127**(13); 6446–6455

Maleki, A. and M. Hamidi (2015). Dissolution Enhancement of a Model Poorly Water-Soluble Drug, Atorvastatin, with Ordered Mesoporous Silica: Comparison of Msf with SBA-15 As Drug Carriers. *Expert Opinion on Drug Delivery*, **13**(2); 171–181

Maleki, A., H. Kettiger, A. Schoubben, J. M. Rosenholm, V. Ambrogi, and M. Hamidi (2017). Mesoporous Silica Materials: From Physico-Chemical Properties to Enhanced Dissolution of Poorly Water-Soluble Drugs. *Journal of Controlled Release*, **262**; 329–347

Mayer, M., M. A. O'Neill, K. E. Murray, N. S. Santos-Magalhães, A. M. A. Carneiro-Leão, A. M. Thompson, and V. C. Appleyard (2005). Usnic Acid: A Non-Genotoxic Compound with Anti-Cancer Properties. *Anti-Cancer Drugs*, **16**(8); 805–809

Okuyama, E., K. Umeyama, M. Yamazaki, Y. Kinoshita, and Y. Yamamoto (1995). Usnic Acid and Diffractaic Acid As Analgesic and Antipyretic Components of Usnea Diffracta. *Planta Medica*, **61**(02); 113–115

Palapa, N. R., N. Ahmad, A. Wijaya, and Z. A. Zahara (2023). Facile Fabrication of Layered Double Hydroxide-Lignin for Efficient Adsorption of Malachite Green. *Science and Technology Indonesia*, **8**(2); 305–311

Shen, S. C., W. K. Ng, L. Chia, Y. C. Dong, and R. B. Tan (2010). Stabilized Amorphous State of Ibuprofen by Co-Spray Drying with Mesoporous SBA-15 to Enhance Dissolution Properties. *Journal of Pharmaceutical Sciences*, **99**(4); 1997–2007

Sokolov, D. N., V. V. Zarubaev, A. A. Shtro, M. P. Polovinka, O. A. Luzina, N. I. Komarova, N. F. Salakhutdinov, and O. I. Kiselev (2012). Anti-Viral Activity of (-)-and (+)-Usnic Acids and Their Derivatives against Influenza Virus A (H1N1) 2009. *Bioorganic & Medicinal Chemistry Letters*, **22**(23); 7060–7064

Supraba, W., Y. Juliantoni, and A. D. Ananto (2021). The Effect of Stirring Speeds to the Entrapment Efficiency in a Nanoparticles Formulation of Java Plum's seed Ethanol Extract (Syzygium cumini). *Acta Chimica Asiana*, **4**(1); 197–103

Thahir, R., A. W. Wahid, N. La Nafie, and I. Raya (2019). Synthesis of Mesoporous Silica SBA-15 through Surfactant Set-Up and Hydrothermal Process. *Rasayan Journal of Chemistry*, **12**(3); 1117–1126

Tng, D. J. H. and J. G. H. Low (2023). Current Status of Silica-Based Nanoparticles As Therapeutics and Its Potential As Therapies against Viruses. *Antiviral Research*, **210**; 105488

Van Speybroeck, M., V. Barillaro, T. Do Thi, R. Mellaerts, J. Martens, J. Van Humbeeck, J. Vermant, P. Annaert, G. Van Den Mooter, and P. Augustijns (2009). Ordered Mesoporous Silica Material SBA-15: A Broad-Spectrum Formulation Platform for Poorly Soluble Drugs. *Journal of Pharmaceutical Sciences*, **98**(8); 2648–2658

Vijayakumar, C., S. Viswanathan, M. K. Reddy, S. Parvathavarthini, A. B. Kundu, and E. Sukumar (2000). Anti-Inflammatory Activity of (+)-Usnic Acid. *Fitoterapia*, **71**(5);

564–566

Vinu, A., T. Mori, and K. Ariga (2006). New Families of Mesoporous Materials. *Science and Technology of Advanced Materials*, **7**(8); 753–771

Wang, Z., B. Chen, G. Quan, F. Li, Q. Wu, L. Dian, Y. Dong, G. Li, and C. Wu (2012). Increasing the Oral Bioavailability of Poorly Water-Soluble Carbamazepine Using Immediate-Release Pellets Supported on SBA-15 Mesoporous Silica. *International Journal of Nanomedicine*, **7**; 5807–5818

Yu, C., B. Tian, J. Fan, G. D. Stucky, and D. Zhao (2001). Salt Effect in the Synthesis of Mesoporous Silica Templated by Non-Ionic Block Copolymers. *Chemical Communications*, (24); 2726–2727

Zaini, E., D. Azhari, and L. Fitriani (2016). Identification and Characterization of Solid Binary System of Quercetin-Nicotinamide. *Oriental Journal of Chemistry*, **32**(3); 1545–1550